Spectrochimica Acta Part A: Molecular and Biomolecular Spectroscopy 271 (2022) 120869

Contents lists available at ScienceDirect

Spectrochimica Acta Part A: Molecular and Biomolecular Spectroscopy

journal homepage: www.elsevier.com/locate/saa

pH-induced changes in Raman, UV–vis absorbance, and fluorescence spectra of dipicolinic acid (DPA)

Dmitry Malyshev [a,1], Rasmus Öberg [a,1], Lars Landström [b], Per Ola Andersson [b,c], Tobias Dahlberg [a], Magnus Andersson [a,d,*]

[a] Dept of Physics, Umeå University, 901 87 Umeå, Sweden
[b] Swedish Defence Research Agency (FOI), Umeå, Sweden
[c] Department of Engineering Sciences, Uppsala University, Uppsala, Sweden
[d] Umeå Centre for Microbial Research (UCMR), Umeå, Sweden

HIGHLIGHTS

- Dipicolinic acid (DPA) protects endospores DNA and are an essential biomarker of bacterial spores.
- DPA can exist in different ionic forms depending on solution pH.
- Raman, absorption and fluorescence spectra of DPA shifts with solution pH.
- The three ionic forms of DPA may have to be considered in spectral analysis and for detection applications.

GRAPHICAL ABSTRACT

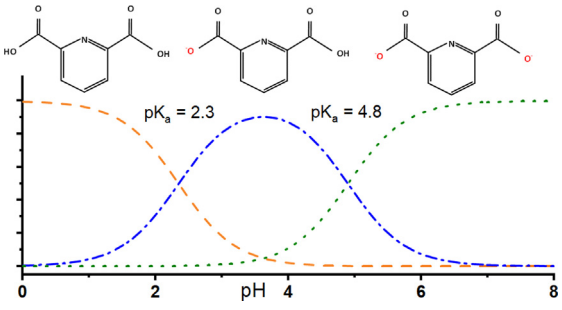

ARTICLE INFO

Article history:
Received 20 August 2021
Received in revised form 29 November 2021
Accepted 5 January 2022
Available online 11 January 2022

Keywords:
Bacterial spores
DPA
Biomarker
Raman spectra
UV–vis absorption spectra
Fluorescence spectra

ABSTRACT

Dipicolinic acid (DPA) is an essential component for the protection of DNA in bacterial endospores and is often used as a biomarker for spore detection. Depending upon the pH of the solution, DPA exists in different ionic forms. Therefore, it is important to understand how these ionic forms influence spectroscopic response. In this work, we characterize Raman and absorption spectra of DPA in a pH range of 2.0–10.5. We show that the ring breathing mode Raman peak of DPA shifts from 1003 cm^{-1} to 1017 cm^{-1} and then to 1000 cm^{-1} as pH increases from 2 to 5. The relative peak intensities related to the different ionic forms of DPA are used to experimentally derive the pK$_a$ values (2.3 and 4.8). We observe using UV–vis spectroscopy that the changes in the absorption spectrum of DPA as a function of pH correlate with the changes observed in Raman spectroscopy, and the same pK$_a$ values are verified. Lastly, using fluorescence spectroscopy and exciting a DPA solution at between 210–330 nm, we observe a shift in fluorescence emission from 375 nm to 425 nm between pH 2 and pH 6 when exciting at 320 nm. Our work shows that the different spectral responses from the three ionic forms of DPA may have to be taken into account in, e.g., spectral analysis and for detection applications.

1. Introduction

Dipicolinic acid (DPA) is a compound that is of interest in, e.g., microbiology and medical diagnostics since it is often considered as a biomarker for bacterial spores [1]. DPA (in its chelated CaDPA form) has been reported to make up to 25 % of the spore core dry

* Corresponding author at: Dept of Physics, Umeå University, 901 87 Umeå, Sweden.
E-mail address: magnus.andersson@umu.se (M. Andersson).
[1] Contributed equally to this work.

https://doi.org/10.1016/j.saa.2022.120869
1386-1425/

weight and protects the bacterial DNA from external stress, such as wet heat [2,3]. Bacterial spores are resilient to environmental hazards and can persist in the environment for years, and may survive common decontamination methods such as ethanol handwash or short term exposure to chlorine based agents like dichloroisocyanurate [4,5]. Thus, pathogenic spores are a major problem in healthcare (e.g., clostridia) and spores like *Bacillus anthracis* (the causative agent of anthrax) are also found listed as biological warfare agents (BWA) [6,7], therefore methods to detect spore biomarkers such as DPA can be useful for rapid detection and tracking of spores [8]. Since DPA is a dicarboxylic acid, it can exist in three different ionization states [9] (Fig. 1) and it is of importance to understand if and how these forms influence a sensor device. Several methods to detect biomarkers exist and of particular interest are rapid and non-invasive approaches such as Raman and fluorescence spectroscopy.

Raman spectroscopy is an analytical and reagentless method that provides a fingerprint of the studied chemical. The technique has been used to study organic molecules [10] and to track chemical changes in bacterial spores [2] as well as the direct release of DPA [2,11]. A major advantage of Raman spectroscopy over other vibrational techniques (e.g., IR spectroscopy) is that water is a weak Raman scatterer, making Raman useful for observing different analytes in aqueous solution. However, reported peak positions and relative intensities for the Raman spectra of, e.g. organic molecules can vary significantly due to differences in sample preparation and laser excitation wavelength. Therefore, reported spectra for biological compounds can differ in published literature [12–15].

For aqueous DPA, Raman peaks are generally reported at 826, 1001, 1387, 1440, and 1572 cm^{-1}, in which the highly prominent peak around 1000 cm^{-1} is typically assigned to the molecule's ring breathing mode [16–20]. There are also studies where the Raman spectrum of aqueous DPA exhibits a double peak of similar intensity at approximately 1000 and 1017 cm^{-1} [21]. DPA in aqueous solution with $CaCl_2$, as well as the main DPA peak found in bacterial spores is generally reported at 1017 cm^{-1}, with the shift attributed to the chelate Ca^{2+} causing a change in the ring breathing mode [18]. In addition to this, there is variation in how the aqueous solutions are prepared. Some studies either use Tris buffer [17,18] to adjust pH to 8.0 and increase solubility and thus signal strength of DPA (which has a solubility of 30 mM in water [22]), and others use NaOH to obtain an approximately neutral solution [16]. There are also studies that report unclear buffer solutions making spectral interpretation and comparison challenging [19,21].

Biomarkers such as DPA may also be detected using fluorescence spectroscopy [23–26]. Previous studies report a broad absorbance band below 300 nm for DPA dissolved in deionised water at concentrations 10 μM at pH 2 [23], and 200 μM at an unknown pH [24]. However, the characteristics of the absorbance band measured from DPA solutions varies in the literature, with some reports showing a double peak around 275 nm at an unknown pH, while other reports show a single, broad peak in the same region at pH 2 [24,25]. Furthermore, Sarasanandarajah et al., show the presence of an additional absorbance peak at shorter wavelengths around 225 nm. In general, prominent fluorescence emission bands were recorded for excitation wavelengths at around 250 and 300 nm [23,24,26]. The origin of the observed emission is investigated and discussed in detail in the references above and, importantly, degradation products are found to strongly influence the overall emission because of their higher fluorescence quantum yield [25]. Regardless of the exact origin of the fluorescence, further knowledge of how pH influences observed fluorescence emission from DPA solutions is valuable for, e.g., bacterial spore detection applications.

To address the above, we characterize how the different ionic forms of DPA influence Raman-, UV–vis absorption-, and fluorescence spectra. We measure the Raman spectrum of DPA at different pH values in both buffered and unbuffered aqueous solutions, and the observed shifts in Raman peak positions and relative intensity as a function of pH are assigned to the different ionic forms. Using the relative abundance of the different forms of DPA as determined by Raman spectra, we experimentally determine the pK_a values of DPA. Lastly, we observe how UV–vis absorption spectra of DPA change with pH, in line with the determined pK_a values, further demonstrating how the ionic forms may have to be considered when performing spectroscopic measurements on DPA. The spectral information given herein can be used to better understand the change in DPA structure, as well as improving indirect methods for bacterial spore detection using DPA as a biomarker.

2. Experimental methods

2.1. Raman-, UV–vis-, and fluorescence systems

To trap spores and acquire Raman spectra we use our optical trap and Laser Tweezers Raman instrument that is assembled around an inverted microscope (IX71, Olympus) [27,28]. A Gaussian laser beam operating at 808 nm (DL808-100-S, CrystaLaser) is coupled into the microscope using a dichroic shortpass mirror with a cut-off wavelength of 650 nm (DMSP650, Thorlabs). Imaging and focusing of the beam is achieved by a 60× water immersion objective (UPlanSApo, Olympus) with a numerical aperture of 1.2 and a working distance of 0.28 mm. The excitation laser power is 20 mW.

The backscattered light is collected by the microscope objective and passed through a notch filter (NF808-34, Thorlabs) to reduce the Rayleigh scattered light. Further, to increase the signal-to-noise ratio, we place a 150 μm diameter pinhole in the focal point of the telescope. Finally, we couple the filtered light into our spectrometer (Model 207, McPherson) through a 150 μm wide entrance slit where an 800 grooves/mm holographic grating disperses the light and the Raman spectrum is captured using a Peltier cooled CCD detector (Newton 920 N-BR-DDXW-RECR, Andor) operated at −95 °C. Our system has a spectral resolution of $<$ 2 cm^{-1} in Raman shift.

We use a UV–vis spectrophotometer (Lambda 650, Perkin Elmer) for absorption measurements, a Fluorescence spectrophotometer (Cary Eclipse, Agilent) for fluorescence measurements, and quartz glass cuvettes (10 mm, Mettler Toledo).

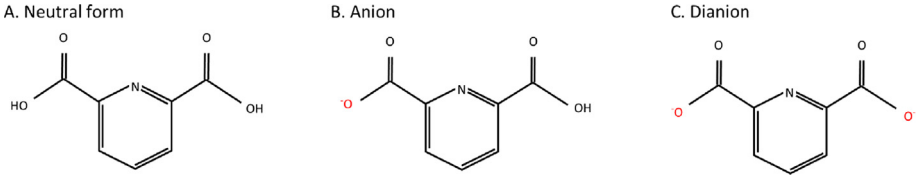

Fig. 1. The neutral, anion, and dianion forms of DPA.

2.2. Sample preparation and measurement

Dipicolinic acid (2,6-Pyridinedicarboxylic acid, 99 %) and buffers (Tris base 99.9 %, Bis-tris 99 %, 3-(Cyclohexylamino)-2-hydroxy-1-propanesulfonic acid (CAPSO) 99 %) were sourced from Sigma Aldrich as dry salts. Additionally, dipicolinic acid (98 %) sourced from Alfa Aesar is used to verify measured spectra. To prepare buffered samples, we first dissolve DPA to a concentration of 0.1 M in a 0.1 M buffer solution. Aliquots of the solution with pH in the range of pH 3.0 (equilibrium pH of the above DPA mixture is 3.0) to pH 10.0 are prepared in steps of 0.5 by adding 5 M NaOH as needed. We measure pH using a Mettler Toledo FiveEasy pH meter and also verify with appropriate pH indicator strips (MQuant). For measurements of DPA in pure aqueous solutions, we dissolve DPA in deionised water to its solubility limit (30 mM at room temperature) and adjust pH from pH 2.0 to pH 10.5.

We prepare the 1:1 calcium chelate DPA solution by following the method described in Kong et al., and mixing 120 mM DPA in Tris buffer with 120 mM $CaCl_2$ (Sigma Aldrich) in Tris buffer [18]. Unbuffered CaDPA (aq.) is prepared by adding 30 mM $CaCl_2$ (aq.) to 30 mM DPA (aq.).

To measure the Raman spectrum of a sample, we place a 10 μl drop between two 0.25 mm thickness quartz cover slips (Alfa Aesar), separated by a 1 mm PDMS ring. We then set the laser focal point at 100 μm above the lower quartz cover slip. The Raman spectrum is recorded using ten accumulations of 10 s in the range of 600–1700 cm^{-1}. We carry out at least three separate measurements for each sample, with figures displaying the average.

To measure the absorbance of DPA in water, we use 3 ml of 300 μM sample solution (100× dilution compared to the Raman measurements) and 3 ml deionised water as a reference. We measure the absorbance, scanning between 210–600 nm with a resolution of 1 nm at a scan speed of 100 nm/min. We carry out at least three separate measurements for each sample, with figures displaying the average.

We measure the fluorescence of DPA in water using 3 ml of 30 mM sample solution by exciting DPA in the 300–330 nm range with 10 nm intervals. The fluorescence emission spectra are measured between 310–600 nm with a resolution of 1 nm and a scan speed of 120 nm/min. Excitation and emission slit width for the measurements both correspond to a 5 nm bandwidth. Additionally, we perform measurements at pH values 2 and 7 using lower concentration sample solutions. We use 10 μM sample solutions excited in the span 210–330 nm with 10 nm intervals to monitor fluorescence peaks and observe potential shifts with pH. At this lower concentration, we note an absorbance <0.2 for wavelengths 220–600 nm, which is low enough to clearly discern fluorescence emissions from a sample. We carry out at least three separate measurements for each sample, with figures displaying average spectra. Additionally, to verify stable emission spectra over successive measurements, we perform 10 successive measurements at excitation wavelengths 220, 250, and 300 nm in solutions with pH values 2 and 7. Lastly, we measure fluorescence from 10 μM fresh DPA sample solutions, alongside samples aged for one and two weeks in a regular lab environment, and a dark environment, respectively. All fluorescence measurements were temperature-controlled at 20°C.

2.3. Data processing

We process Raman spectra using an open-source Matlab script provided by the Vibrational Spectroscopy Core Facility, Umeå University [29]. To baseline correct the spectra we use an asymmetrical least squares algorithm [30] with $\lambda = 10^4$ and $p = 10^{-3}$. We smooth spectra using a Savitzky-Golay filter [31] of polynomial order 1 and a frame rate of 5. We fitted Voigt peaks to Raman spectra using Fityk 1.3.1 and graphs were plotted in Origin 2018 (OriginLab). Fluorescence excitation and emission spectra are corrected to account for the lamp emission profile and response function of the fluorescence spectrophotometer.

3. Results and Discussion

3.1. DPA Raman spectrum changes with pH

To measure pH-induced changes in DPA, we use our micro-Raman setup and first measured Raman spectra of DPA in three different buffer solutions: Bis-tris, Tris, and CAPSO. We show Raman spectra of the pure buffers in Fig. S1. The buffer allows us to more easily control changes in the pH of the solution and also allow for a higher solubility of DPA. 0.1 M DPA in 0.1 M Bis-tris buffer results in an equilibrium pH of 3.0 and the corresponding DPA Raman spectrum clearly shows the typical characteristic peaks at 1017 cm^{-1} and 1603 cm^{-1} (top spectrum in Fig. 2). We thereafter increase the pH of the DPA in Bis-tris buffer solution in steps of 0.5. As the pH increases, we note that the 1017 cm^{-1} peak and 1603 cm^{-1} peaks gradually decrease, and at pH 6.0, these two peaks are no longer distinguishable. Meanwhile, three other peaks at 1000, 1430 and 1575 cm^{-1}, increase over the same pH range. These peaks have previously been assigned as the ring breathing mode, the C-C ring stretch and ring stretch, respectively [20,18]. Thus, the observed change in the DPA Raman spectrum reflects the change in molecular structure as the pH varies between 3.0 and 6.0. From pH 6.0 to 10.0, no significant change in the spectrum can be observed, with only slight variations when changing between buffers at pH 7.0 and 9.0, as shown in Fig. S2. This implies that no change in the ionic structure occurs between pH 6–10.

To verify that the changes in peak intensities are indeed due to a change in the form of DPA, we track how peak intensity changes with pH in pure aqueous solutions. The signal intensity in unbuffered solution is lower due to the lower solubility of DPA in water (30 mM, as measured at room temperature), but its naturally lower pH makes it easier to observe the change in Raman peaks from pH 2.0 and upward. Observing this wider pH-span, we plot the relative intensities of the 1000, 1003, and 1017 cm^{-1} Raman peaks, see Fig. 3A. The peaks at around 1000 and 1003 cm^{-1} together with the 1017 cm^{-1} peak are shown in detail in Fig. 3B. At low pH, the dominant peak is at 1003 cm^{-1}, which at around pH 3.5 shifts to about 1000 cm^{-1}. Similar behaviour can also be seen in buffered DPA, however, the peak shift from 1003 to 1000 cm^{-1} is less clearly observed due to the neutral form being dominant at lower pH values and not fully resolved at pH 3 (as limited by the buffer solution).

Another peak shift observable in pure aqueous solution is the 1575 cm^{-1} peak, which shifts to approximately 1580 cm^{-1} in a similar manner to the 1000–1003 cm^{-1} peak shift. This follows the reported assignment of the 1575 cm^{-1} peak as ring stretch, closely related to the ring breathing mode around 1000 cm^{-1}. However, it is more difficult to quantify the changes in intensity with the ring stretch peak shift due to the low peak prominence of the 1575 cm^{-1} peak in unbuffered solution, and lack of low pH data points in buffered solution.

As a dicarboxylic acid, DPA is expected to have two pK_a values, and potentially one third for the pyridine group at very low pH (the isoelectric point predicted at pH 0.8 [9]). However, the reported pK_a values for DPA in the literature vary considerably, with values of 2.16/6.92 [32] listed in a research article, values of 0.55/7.02 [33], −2.5/3.24 [34] from internet databases and a predicted 3.29/4.01 based on the molecule on Chemicalize [9]. In addition, there is also a reported value of 2.25/4.4 [35] for CaDPA. Given

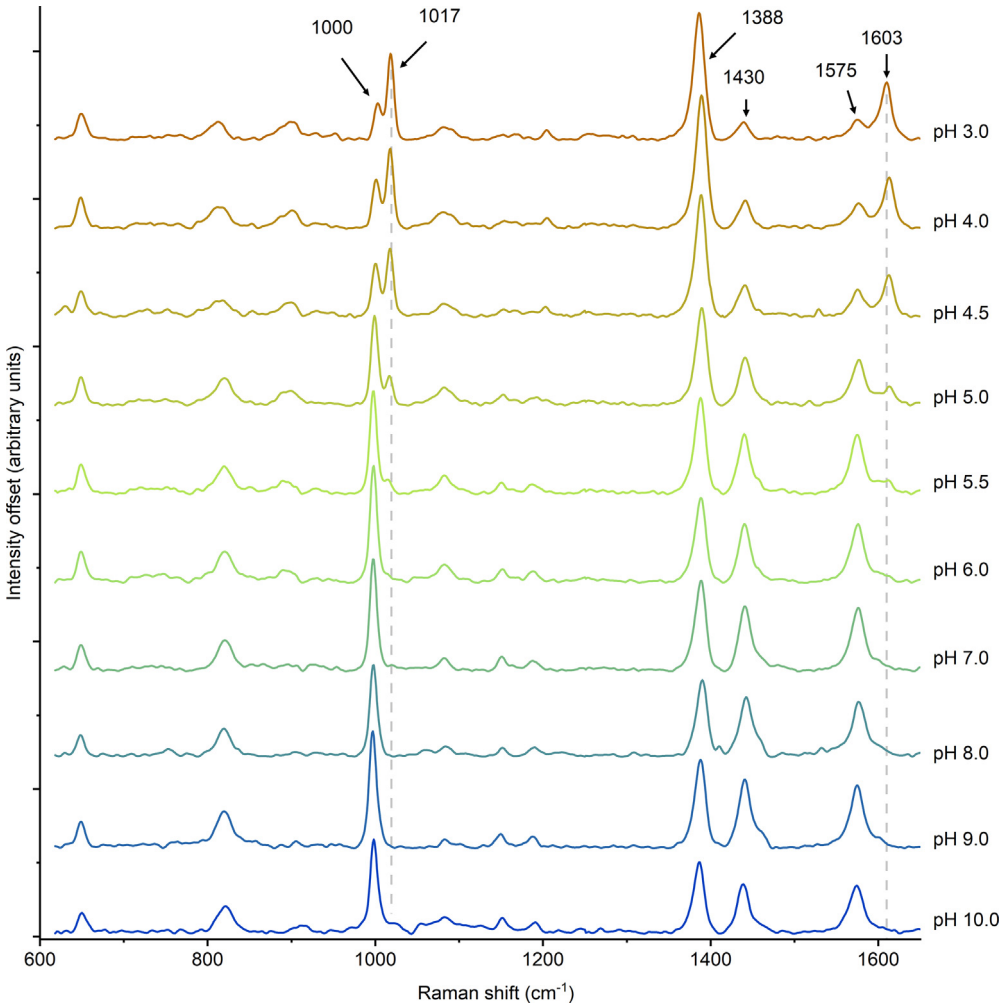

Fig. 2. Raman spectra of DPA in Bis-tris (pH 3–7), Tris (pH 8–9) and CAPSO (pH 10) aqueous buffers for the pH range 3.0–10.0. The two regions with significant spectral changes (1017 and 1603 cm^{-1}) are indicated with dashed lines. Vertical axis is the spectral intensity given in arbitrary units.

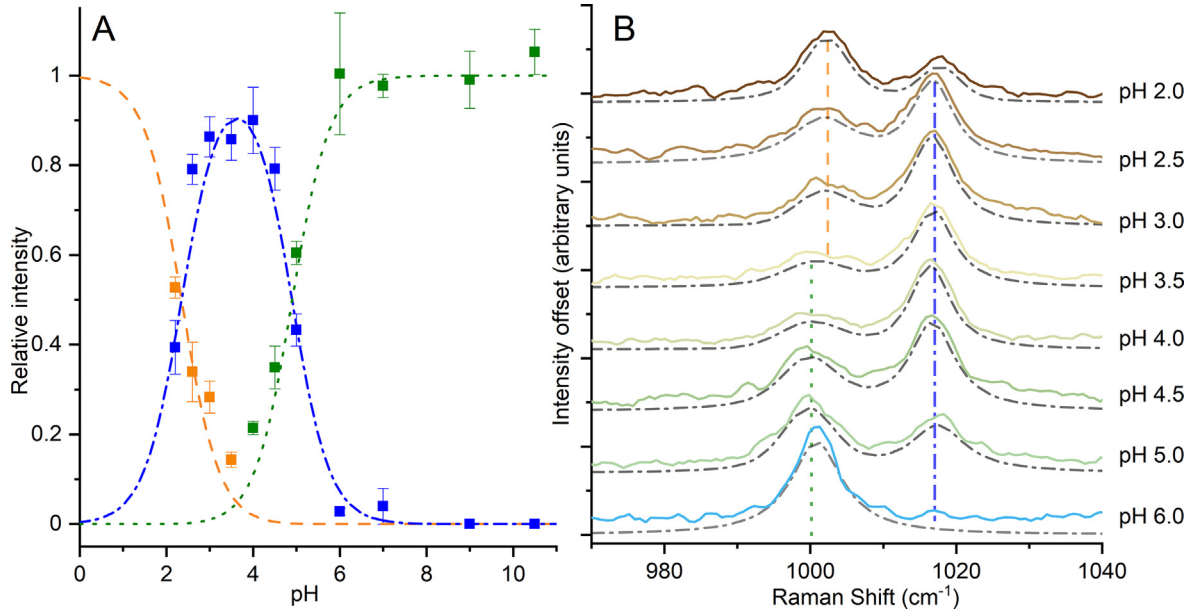

Fig. 3. A) Change in relative intensities of the 1003 cm^{-1} (in orange), 1000 cm^{-1} (in green) and the 1017 cm^{-1} (in blue) peaks of DPA in unbuffered DPA aqueous solutions. Dashed lines show the relative abundance of the different forms of DPA calculated for pK_a values of 2.3 and 4.8. The experimental measurements fit the predicted values for the 1017 cm^{-1} peak being being assigned to the anion, and the 1000–1003 cm^{-1} peak being the sum of the neutral (1003 cm^{-1}) and dianion (1000 cm^{-1}) peaks. B) The 970–1040 cm^{-1} region of the Raman spectrum for DPA dissolved in water during the transition of the 1000/1003 cm^{-1} peaks. The measured spectra are in color, while the fitted peaks are in grey. The dashed vertical lines at 1000, 1003 and and 1017 cm^{-1} are added to more clearly illustrate the shift of the 10003 cm^{-1} peak with increasing pH.

the disparity in these numbers, having a clearly determined value is important and we can derive the pK_a values from our data based on the relative intensities of the peaks. We find that our data aligns best when fitted to the pK_a values of 2.3 and 4.8 (Fig. 3A, dashed and dotted lines), which is different from other reported values, but closest to the one reported by Tang et al. [35]. The difference is likely due to the difference in the chelate form of DPA studied compared to non chelated DPA. This also highlights the need for clearly sourced values for such data. From the fitted pK_a values and measured relative intensities, we can assign the three peaks discussed above to the different ionic forms of DPA as neutral (orange), anion (blue), and dianion (green) as shown in Fig. 3.

In our measurements, we confirm that at equilibrium pH 8, CaDPA in aqueous solution has the most intense peak at 1017 cm^{-1} (Fig. S5), matching the spectrum reported in previously published works [17,18]. We also recorded the Raman spectrum of the powder form of DPA (Fig. S4), which is also consistent with previously reported spectra [18]. As noted earlier, the 1000–1017 cm^{-1} region peaks in the Raman spectrum of DPA are assigned as ring breathing modes, though they were also described as a combination peak arising from the addition of the ring breathing and ring bending modes in *meta*-substituted benzenes [36]. The difference in the peak in the CaDPA (DPA in solution with Ca^{2+}) compared to DPA was reported to be caused by the strong interaction from the chelate Ca^{2+} ion, which forms relatively strong bonds with both hydroxyl groups, putting stress on the ring itself [18]. It is notable that CaDPA has the same 1017 cm^{-1} peak as the anion from of non chelated DPA 3B (pH 2.5–4.5). Both the neutral form and the dianion are symmetric in their charge distribution and have similar peak locations at 1003 and 1000 cm^{-1}, while the anion has asymmetric charge distribution which can influence the ring breathing mode.

3.2. UV-absorption and fluorescence spectroscopy characterization of DPA in aqueous solutions with different pH

The earlier described and discussed Raman spectroscopy study relates to molecular vibrational modes of dissolved DPA and how pH variations alter the molecule and associated modes. The DPA molecules can then be assumed to be in their electronic singlet ground state S_0. To complement the vibrational mode studies above, we also applied electronic spectroscopy to study spectral profiles of UV absorbance (210–330 nm) and fluorescence emission (220–500 nm) by UV excitation on DPA solutions with different concentrations and pH.

As seen in absorption spectra displayed in Fig. 4A, and in greater detail in Figs. S6-S8, areas of interest are found in the UV region, with pH-induced changes in the absorbance around 270, 225, and 215 nm, respectively. We find no measurable absorbance at wavelengths longer than ~325 nm, and no significant change in the absorption spectrum is seen for higher pH values (7–11). The spectral response between 240 and 300 nm (obtained at pH 7) agrees well with literature data found for aqueous DPA solution at pH 7.5 [26,23], and also with recently published spectra by Nardi et al., on DPA and on dimethyl dipicolinate ester (DMDP) in deaerated MeCN:H_2O (9:1 vol/vol), where the latter spectrum also includes shorter wavelengths down to 210 nm [25].

A careful spectroscopic and theoretical investigation of the photophysics of CaDPA has recently been undertaken by Mundt et al. [26]. From quantum chemical computations, the electronic absorption associated with a maximum of around 270 nm is assigned to a singlet–singlet transition from S_0 to S_3. The absorption maximum centered around 225 nm is attributed to the transition from ground state to higher allowed singlet states involving π electrons. Other excited states, including forbidden states, are also identified and described. Although we expect the DPA to exhibit similar photophysics to its CaDPA form as reported by Mundt *et al.*, the lack of chelate in DPA is likely to influence its photophysics. Furthermore, the variation of the ionic form in DPA with pH would influence the electronic structure of the molecule, and thus its spectroscopic response. As the pH of the DPA solution is altered while keeping the concentration constant, we observe a change in the intensity of the various absorbance bands seen in Fig. 4A. These changes are further illustrated in Fig. 4B, showing the normalized intensity of the absorbance bands relative to their maximum and minimum values in the measured pH range. For lower pH values (pH 2–3), we

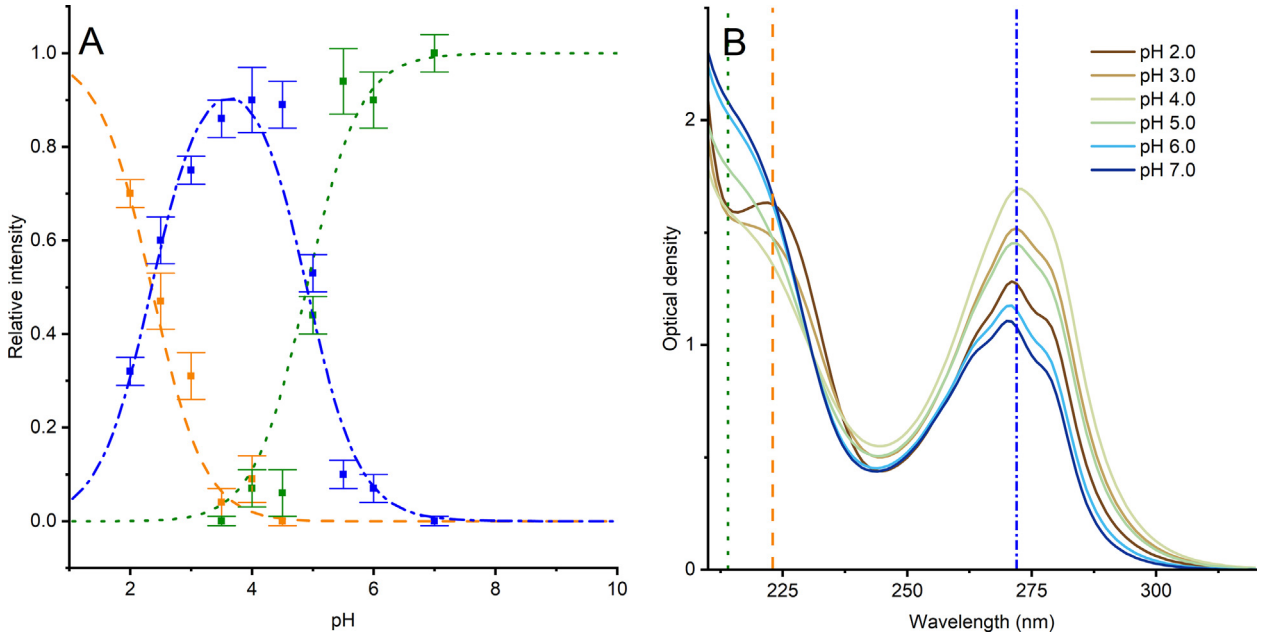

Fig. 4. A) Absorption spectra of 300 μM DPA in the pH range from pH 2.0 to pH 7.0. As pH increases, the relative intensity maximum shifts from 225 nm to 270 nm, and is then followed by an increase in absorbance around 215 nm. These wavelengths of interest are marked with coloured dashed and dotted lines. B) Normalized absorbance relative their maximum and minimum measured values (scatter points) of the 225 (orange), 270 (blue), and 215 nm (green) DPA solution absorbance areas of interest. These changes correspond well to the calculated relative abundance of ionization states of DPA using previously fitted pK_a values (corresponding lines).

observe an absorbance peak/shoulder at 225 nm that partially diminishes as the pH of the solution increases and vanishes at around pH 4 (orange), where we in turn see an increase in the absorbance peak around 270 nm (blue), and the vibronic structure (shoulders around 260 and 285 nm) is less pronounced and nearly unresolved. Beyond pH 4 the absorbance peak around 270 nm diminishes and the spectrum again displays vibronic details. Finally, for pH 5–7 we observe a resurgence in absorbance at shorter wavelengths, however, the absorbance peak appears blue-shifted with a shoulder around 215 nm (green). Comparing the relative change in absorbance at three wavelengths as a function of pH to the calculated relative abundance of the three forms using pK_a values derived from Raman measurements (matching color dashed and dotted lines), we observe them to be largely identical. From this, we conclude that the absorption spectrum of DPA depends directly on its ionic form (pH in an aqueous solution).

To assess how excitation wavelength and pH impacts fluorescence emission spectra, we measure fresh DPA and DPA aged for one week at pH 2 and 7. A brief qualitative analysis of freshly prepared samples (aged a few minutes) and aged for one and two weeks are discussed further down in this section. For aged DPA, we observe three emission regions when analyzing 10 μM sample solutions; excitation in the 220 nm range yields an unstructured fluorescence emission band with a maximum varying between 290–310 nm (Fig. S9A). Excitation in the 250 range yields a fluorescence emission around 350 nm (Fig. S9B). These two excitation regions do not show any pH dependency. However, when excited at the 300 nm range the DPA solution displays a significant pH-dependent fluorescence emission, showing a maximum at 380 and 430 nm for pH 2 and 7, respectively (Fig. S10).

The corresponding fluorescence excitation spectra from fresh DPA solution show three maxima measured at different emission wavelengths (λ_{em}). When λ_{em} is set to 300 and 350 nm, both excitation spectra show two distinct maxima centred about 220 and 260 nm (Fig. S11). The 220 nm band dominates at λ_{em} = 300 nm while the 260 nm band is more intense at λ_{em} = 350 nm. The former excitation spectrum overlaps better with the corresponding UV-ABS spectrum (Fig. 4A) than the latter, interpreted as a higher content of DPA fluorescence is recorded at 300 nm rather than at 350 nm, and that other species, likely degradation products of DPA, dominate the emission around 350 nm. Moreover, in the excitation spectrum, the maximum at shorter wavelengths shifts from 220 to 230 nm when changing λ_{em} from 300 to 350 nm, also indicating that different fluorescent species are present in the sample solution. Excitation bands recorded from fluorescence at 380 (pH 2) and 430 nm (pH 7) of fresh 10 μM samples, both show a maximum excitation at 325 nm, while the second peak located at 260 nm clearly differs in intensity (Fig. S11). The band at 325 nm is highly fluorescent, lies outside DPA absorbance region and is not dependent on pH (in the interval pH 2 - pH 7), suggesting that this fluorescence band may instead originate from a degradation product (with a higher fluorescent yield) rather than DPA itself.

While interpreting fluorescence data, both photophysical and photochemical effects of DPA in aqueous solutions have to be considered. The fluorescence quantum yield of DPA in solutions is very low, on the order of 10^{-5} as presented in a thorough work on the photophysics of DPA by Mundt et al. [26]. DPA dissolved in D_2O at pH 8 shows a broad fluorescence emission band without fine structure after excitation at 255 nm. After excitation to the S_3 state the molecule relaxes to the ground state mainly by non-radiative pathways via internal conversions to lower energy singlet excited states and intersystem crossing to lower energy triplet states. The photophysical properties are challenging to study and characterize because of the photoinstability of DPA [25,23,24] in aqueous solutions associated with the rapid degradation kinetics, occurring in the span of minutes [25]. A recent spectroscopic study aimed at characterizing DPA and its photoproducts by Nardi et al., explore the phosphorescence behaviour and identify photoproducts based on bipyridine structures [25]. As they point out, these degradation products exhibit higher fluorescence emission yields than DPA, i.e., they likely contribute significantly to the fluorescence spectral response of aqueous DPA samples, especially when aged samples are studied.

Based on the above data and considering the scope of this paper, we herein only perform a brief qualitative analysis of the measured fluorescence data from freshly prepared samples (aged a few minutes) and aged for one and two weeks. One batch (containing samples of pH 2 and 7) was stored in darkness while the other one (also pH 2 and 7) was exposed to ordinary indoor ambient light. We observe no difference in fluorescence spectra between the two and again, three spectral fluorescence regions can be seen. Ageing has a strong effect on the spectral profiles (Fig. S9-10), especially for excitation at 300–330 nm where the fluorescence intensity increases for the aged samples. When excited at 300–330 nm the fluorescence spectra were of higher intensity in samples of pH 7 than those of pH 2, again indicating that different structures are present. In other words, since we are exciting the sample solution outside the DPA absorption spectrum (or at the edge of the red wing), and light exposure does not appear to influence the ageing process, we are most likely observing emission from solvent-imposed degradation products which in turn seem to follow certain pH dependence.

To further study the pH dependent fluorescence emissions from DPA obtained by 300–330 nm excitation, we use high concentration solutions (30 mM), i.e., the same concentration as for the Raman experiments described earlier. 30 mM is a very high concentration for fluorescence studies and is only considered due to the low absorbance of DPA at these excitation wavelengths. The corresponding absorbance in this wavelength range is shown in Fig. S12, and does not indicate any new (abnormal) absorption bands at the red part of the spectrum. Rather the absorbance could be regarded as higher absorbance equivalents of Fig. 4A. Measuring the fluorescence emission from this higher concentration solution excited at 320 nm, we observe a redshift of the fluorescence emission maximum from 380 nm at pH 2 to 430 nm at pH 6, as seen in Fig. 5. No further change in the emission spectrum occurs at higher pH values (7–11). Excitation at both shorter and longer

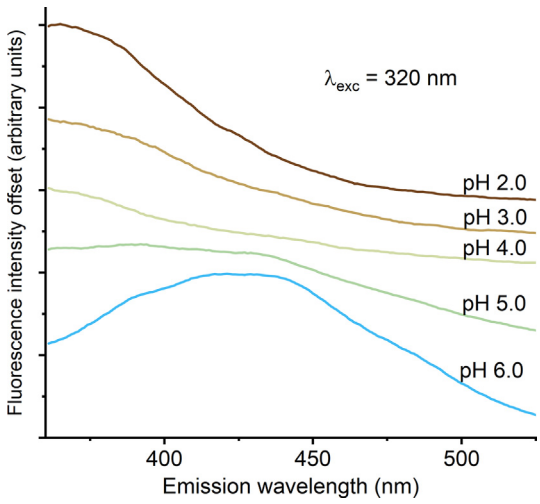

Fig. 5. Emission spectra from 30 mM DPA as pH increases from 2.0 to 6.0. As pH increases, the emission peak shifts from around 380 nm to 430 nm. Excitation wavelength (λ_{exc}) is 320 nm.

wavelengths yields weaker emission spectra, with the loss of emission at shorter wavelengths due to self-absorbance by the DPA solution. In line with the earlier established pK_a values for DPA this pH dependence may suggest that the two bands at ~380 nm and ~430 nm correspond to the neutral and dianion form of DPA, respectively. However, it is more plausible that the observed shift arises from degradation products of DPA. Nardi et al., identified different photoproducts that are structurally related to bipyridine derivates, with two carboxyl groups similar to DPA, and thus neutral, anionic and dianionic forms dependent on the pH of the solution.

4. Conclusion

DPA is an essential component for bacterial spores and can be used as a biomarker for spore detection based on optical spectroscopy techniques [1,8,21]. As DPA is a dicarboxylic acid, the pH of an aqueous solution determines the ratio of the ionic forms, and consequentially the spectroscopic response. In addition, degradation effects may also affect the overall spectral result.

The results in this work improve our understanding of DPA in relation to solution pH, and can be used to explain differences seen in spectra. Using Raman spectroscopy and 808 nm excitation, we show that the DPA ring breathing mode peak can be present at three Raman shifts (1003, 1017 and 1000 cm^{-1}), corresponding to different ionization states of DPA. From the relative intensities of these peaks, we fit the pK_a values of DPA, which have previously been reported at different values, to be 2.3 and 4.8. We further verify these pK_a values using UV–vis absorption spectroscopy which similarly displays three separate absorbance bands (225, 270 and 215 nm) corresponding to the neutral, anion and dianion forms. Lastly, we find a pH dependence in the fluorescence expressed by a DPA solution excited at 300 nm for 10 μM and at 320 nm for 30 mM, with the fluorescence emission peak centered at 380 and 430 nm at pH values 2.0 and 6.0, respectively. However, observing a large increase in the emission spectra intensity in DPA solutions aged one week compared to those from fresh solutions, these peaks likely correspond to degradation products in different ionic forms.

The results in this study can also be seen in the context of using spectroscopy techniques for detecting spores and traces of spores in "real world" environments such as hospitals. Disinfection agents such as sodium hypochlorite and most soaps are relatively high pH, while other peroxygen based disinfectants, such as peracetic acid or hydrogen peroxide would have lower pH [37–39]. In this environment, it would be important to account for the pH of the surface.

Overall, this study highlights the importance of accounting for pH-induced effects when using spectroscopy to measure spores and spore components in aqueous solutions, e.g., as DPA is often considered as a biomarker for its potential in rapid, indirect detection of spores.

Declaration of Competing Interest

The authors declare that they have no known competing financial interests or personal relationships that could have appeared to influence the work reported in this paper.

Acknowledgements

This work was supported by the Swedish Research Council (2019–04016); the Umeå University Industrial Doctoral School (IDS); Kempestiftelserna (JCK-1916.2); and Swedish Department of Defence, Project No. 470-A400821.

Appendix A. Supplementary material

Supplementary data associated with this article can be found, in the online version, at https://doi.org/10.1016/j.saa.2022.120869.

References

[1] H. Shibata, S. Yamashita, M. Ohe, I. Tani, Laser Raman spectroscopy of lyophilized bacterial spores, Microbiol. Immunol. 30 (1986) 307–313.
[2] P. Zhang, L. Kong, P. Setlow, Y.-Q. Li, Characterization of Wet-Heat Inactivation of Single Spores of Bacillus Species by Dual-Trap Raman Spectroscopy and Elastic Light Scattering, Appl. Environ. Microbiol. 76 (2010) 1796–1805.
[3] M. Laue, H.-M. Han, C. Dittmann, P. Setlow, Intracellular membranes of bacterial endospores are reservoirs for spore core membrane expansion during spore germination, Scient. Rep. 8 (2018) 11388.
[4] G.C. Stewart, The Exosporium Layer of Bacterial Spores: a Connection to the Environment and the Infected Host, Microbiol. Mol. Biol. Rev. 79 (2015) 437–457.
[5] C. Dyer, L.P. Hutt, R. Burky, L.T. Joshi, Biocide Resistance and Transmission of Clostridium difficile Spores Spiked onto Clinical Surfaces from an American Health Care Facility, Appl. Environ. Microbiol. 85 (2019) 1–11.
[6] R.J. Manchee, M.G. Broster, I.S. Anderson, R.M. Henstridge, J. Melling, Decontamination of Bacillus anthracis on Gruinard Island?, Nature 303 (1983) 239–240
[7] A.K. Goel, Anthrax: A disease of biowarfare and public health importance, World J. Clin. Cases 3 (2015) 20.
[8] S. Wang, J. Yu, M. Suvira, P. Setlow, Y.-Q. Li, Uptake of and Resistance to the Antibiotic Berberine by Individual Dormant, Germinating and Outgrowing Bacillus Spores as Monitored by Laser Tweezers Raman Spectroscopy, PLOS ONE 10 (2015) e0144183.
[9] Chemicalize, developed by chemaxon (http://www.chemaxon.com), used 18/05/2021, 2021. URL: https://chemicalize.com/.
[10] N.B. Colthup, L.H. Daly, S.E. Wiberley, Aromatic and Heteroaromatic Rings, Introduction to Infrared and Raman, Spectroscopy 225 (1990) 261–288.
[11] L. Kong, P. Zhang, G. Wang, J. Yu, P. Setlow, Y.Q. Li, Characterization of bacterial spore germination using phase-contrast and fluorescence microscopy, Raman spectroscopy and optical tweezers, Nat. Protoc. 6 (2011) 625–639.
[12] S.M. Angel, N.R. Gomer, S.K. Sharma, C. McKay, Remote Raman Spectroscopy for Planetary Exploration: A Review, Appl. Spectrosc. 66 (2012) 137–150.
[13] P.T. Freire, F.M. Barboza, J.A. Lima, F.E. Melo, J.M. Filho, Raman Spectroscopy of Amino Acid Crystals, Raman Spectroscopy and Applications (2017).
[14] A.L. Jenkins, R.A. Larsen, T.B. Williams, Characterization of amino acids using Raman spectroscopy, Spectrochim. Acta Part A Mol. Biomol. Spectrosc. 61 (2005) 1585–1594.
[15] J. Chen, H. Cheng, X. Zhu, L. Jin, H. Zheng, In situ transformation of an aqueous amino acid at high pressures and temperatures, Geochem. J. 41 (2007) 283–290.
[16] D. Pestov, M. Zhin, Z.E. Sariyanni, N.G. Kalugin, A.A. Kolomenskii, R. Murawski, G.G. Paulus, V.A. Sautenkov, H. Schuessler, A.V. Sokolov, G.R. Welch, Y.V. Rostovtsev, T. Siebert, D.A. Akimov, S. Graefe, W. Kiefer, M.O. Scully, Visible and UV coherent Raman spectroscopy of dipicolinic acid, Proceedings of the National Academy of Sciences of the United States of America 102 (2005) 14976–14981.
[17] S.-S. Huang, D. Chen, P.L. Pelczar, V.R. Vepachedu, P. Setlow, Y.-Q. Li, Levels of Ca2+-Dipicolinic Acid in Individual Bacillus Spores Determined Using Microfluidic Raman Tweezers, J. Bacteriol. 189 (2007) 4681–4687.
[18] L. Kong, P. Setlow, Y.-Q. Li, Analysis of the Raman spectra of Ca2+-dipicolinic acid alone and in the bacterial spore core in both aqueous and dehydrated environments, The Analyst 137 (2012) 3683.
[19] A. Kolomenskii, H. Schuessler, Raman spectra of dipicolinic acid in crystalline and liquid environments, Spectrochim. Acta Part A Mol. Biomol. Spectrosc. 61 (2005) 647–651.
[20] K. McCann, J. Laane, Raman and infrared spectra and theoretical calculations of dipicolinic acid, dinicotinic acid, and their dianions, J. Mol. Struct. 890 (2008) 346–358.
[21] E. Kočišová, M. Procházka, Drop coating deposition Raman spectroscopy of dipicolinic acid, J. Raman Spectrosc. 49 (2018) 2050–2052.
[22] Pubchem database, 2,6-pyridinedicarboxylic acid, accessed 8/05/2021, 2021. URL: https://pubchem.ncbi.nlm.nih.gov/compound/2_6-Pyridinedicarboxylic-acid.
[23] R. Nudelman, B.V. Bronk, S. Efrima, Fluorescence emission derived from dipicolinic acid, its sodium, and its calcium salts, Appl. Spectrosc. 54 (2000) 445–449.
[24] S. Sarasanandarajah, J. Kunnil, B.V. Bronk, L. Reinisch, Two-dimensional multiwavelength fluorescence spectra of dipicolinic acid and calcium dipicolinate, Appl. Opt. 44 (2005) 1182–1187.
[25] G. Nardi, M. Lineros-Rosa, F. Palumbo, M.A. Miranda, V. Lhiaubet-Vallet, Spectroscopic characterization of dipicolinic acid and its photoproducts as thymine photosensitizers, Spectrochim. Acta - Part A: Mol. Biomol. Spectrosc. 245 (2021) 118898.
[26] R. Mundt, C. Torres Ziegenbein, S. Fröbel, O. Weingart, P. Gilch, Femtosecond spectroscopy of calcium dipicolinate - A major component of bacterial spores, J. Phys. Chem. B 120 (2016) 9376–9386.

[27] T. Stangner, T. Dahlberg, P. Svenmarker, J. Zakrisson, K. Wiklund, L.B. Oddershede, M. Andersson, Cooke-Triplet tweezers: more compact, robust, and efficient optical tweezers, Opt. Lett. 43 (2018) 1990.
[28] T. Dahlberg, D. Malyshev, P.O. Andersson, M. Andersson, Biophysical fingerprinting of single bacterial spores using laser Raman optical tweezers, Proc. SPIE 11416, Chemical, Biological, Radiological, Nuclear, and Explosives (CBRNE) Sensing XXI, 2020
[29] Vibrational spectroscopy core facility, accessed 8/04/2021, 2021. URL: https://www.umu.se/en/research/infrastructure/visp/downloads/.
[30] P.H.C. Eilers, Parametric Time Warping, Anal. Chem. 76 (2004) 404–411.
[31] M.J.E. Savitzky, A.; Golay, Smoothing and Differentiation, Anal. Chem 36 (1964) 1627–1639.
[32] S. Farquharson, A. Gift, P. Maksymiuk, F.E. Inscore, W.W. Smith, pH dependence of methyl phosphonic acid, dipicolinic acid, and cyanide by surface-enhanced Raman spectroscopy, in: Proc. SPIE, 5269, Chemical and Biological Point Sensors for Homeland Defense, 2004.
[33] Drugbank database, 2,6-pyridinedicarboxylic acid, accessed 8/04/2021, 2021. URL: https://go.drugbank.com/drugs/DB04267.
[34] Foodb database, 2,6-pyridinedicarboxylic acid, accessed 8/04/2021, 2021. URL: https://foodb.ca/compounds/FDB011167.
[35] T. Tang, K. Rajan, N. Grecz, Mixed Chelates of Ca(II)-Pyridine-2,6-Dicarboxylate with Some Amino Acids Related to Bacterial Spores, Biophys. J . 8 (1968) 1458–1474.
[36] N.B. Colthup, L.H. Daly, S.E. Wiberley, Vibrational and Rotational Spectra, Introduction to Infrared and Raman, Spectroscopy (1990) 1–73.
[37] P. Stewart, J. Rayner, F. Roe, W. Rees, Biofilm penetration and disinfection efficacy of alkaline hypochlorite and chlorosulfamates, J. Appl. Microbiol. 91 (2001) 525–532.
[38] M. Kitis, Disinfection of wastewater with peracetic acid: a review, Environ. Int. 30 (2004) 47–55.
[39] M. McFadden, J. Loconsole, A. Schockling, R. Nerenberg, J. Pavissich, Comparing peracetic acid and hypochlorite for disinfection of combined sewer overflows: Effects of suspended-solids and pH, Sci. Total Environ. 599–600 (2017) 533–539.